Journal of Solid State Chemistry 219 (2014) 179–184

Contents lists available at ScienceDirect

Journal of Solid State Chemistry

journal homepage: www.elsevier.com/locate/jssc

Short-range order in Fe-based metallic glasses: Wide-angle X-ray scattering studies

Rafał Babilas [a,*], Łukasz Hawełek [b,c], Andrzej Burian [c]

[a] Institute of Engineering Materials and Biomaterials, Silesian University of Technology, Gliwice, Poland
[b] Institute of Non-Ferrous Metals, Gliwice, Poland
[c] A. Chelkowski Institute of Physics, University of Silesia, Katowice, Poland

ARTICLE INFO

Article history:
Received 20 May 2014
Received in revised form
19 July 2014
Accepted 23 July 2014
Available online 1 August 2014

Keywords:
Amorphous materials
Fe-based metallic glasses
Atomic scale structure
Wide-angle X-ray scattering

ABSTRACT

The local atomic structure of the $Fe_{80}B_{20}$, $Fe_{70}Nb_{10}B_{20}$ and $Fe_{62}Nb_{8}B_{30}$ glasses prepared in the form of ribbons has been studied by wide-angle X-ray scattering. Structural information about the amorphous ribbons has been derived from analysis of the radial distribution functions using the least-squares curve-fitting method. The obtained structural parameters indicate that Fe–Fe, Fe–B, Fe–Nb and Nb–B contributions are involved in the near-neighbor coordination spheres. The possible similarities of the local atomic arrangement in the investigated glasses and the crystalline Fe_3B, $Fe_{23}B_6$ and bcc Fe structures are also discussed.

1. Introduction

Amorphous metallic alloys, also called metallic glasses, have attracted considerable attention since it was shown that they have interesting properties such as mechanical strength, great wear and corrosion resistance [1]. Fe-based metallic glasses exhibit good soft magnetic properties that make them promising as a new type of ferromagnetic materials. However their preparation requires high critical cooling rates [2]. Physical properties and the glass-forming ability of these materials are dependent on their chemical composition. The addition of transition metals such as Nb or Zr to the Fe–B based system modifies the liquid structure by changing the atomic packing configurations, that extends supercooled liquid region (ΔT_x) – evaluating factor of the amorphous structure stability [3]. In the present work studies of the short-range atomic arrangement in the binary $Fe_{80}B_{20}$ and ternary $Fe_{70}B_{20}Nb_{10}$, $Fe_{62}B_{30}Nb_{8}$ metallic glasses are presented.

2. Material and methods

The $Fe_{80}B_{20}$ and $Fe_{70}B_{20}Nb_{10}$, $Fe_{62}B_{30}Nb_{8}$ metallic glasses were prepared in the form of ribbons with thickness of 0.03 mm and width of 5 mm. First, ingots were obtained by induction melting of pure element mixtures of Fe (99.98%), B (99.9%) and Nb (99.95%) in the proper proportions. Then the glassy ribbons were prepared by the "chill-block melt spinning" technique in the argon protective atmosphere. In this method of continuous casting the liquids are rapidly quenched on the surface of a turning copper wheel [4–7]. The casting conditions were the linear speed of the copper wheel 20 m/s and ejection overpressure of the molten alloy under the Ar (99.96%) atmosphere 0.04 MPa.

The amorphous structure of the as-prepared samples was tested by the X-ray diffraction technique in reflection mode using the Seifert-FPM XRD 7 diffractometer with Co $K\alpha$ radiation (wavelength = 1.7902 Å). The densities of the studied alloys were determined using the Archimedean method.

The wide-angle X-ray scattering measurements were carried out using the powder Rigaku-Denki D/MAX RAPID II-R diffractometer equipped with a rotating Ag anode (wavelength = 0.5608 Å), a flat (002) graphite monochromator mounted in the incident beam and a 2D detector in the form of an image plate in the Debye–Scherrer geometry. The samples, powdered in an agate mortar, were placed for the measurements inside special glass capillaries of about 0.5 mm in diameter and with a wall thickness of 0.01 mm. The beam size at the sample was 0.3 mm. The diffraction patterns of the sample filled and empty capillaries were recorded and then the intensity of the empty capillary was subtracted from the total intensity. The 2D diffraction data were converted to the 1D intensity using suitable software. The experimental raw data were corrected for background, fluorescence, Compton scattering, polarization

---

* Corresponding author.
E-mail address: rafal.babilas@polsl.pl (R. Babilas).

http://dx.doi.org/10.1016/j.jssc.2014.07.034
0022-4596/

and absorption and then normalized to the electron units using the high-angle method [8,9]. The data were recorded in the scattering vector range between 0.5 and 22 $Å^{-1}$. The scattering vector Q is defined as the difference between the wave vectors, each with the magnitude $2\pi/\lambda$, in the directions of the incident and scattered beam, respectively. $Q=4\pi \sin\theta/\lambda$, where 2θ is the angle between the incident and scattered beam, λ is the wavelength.

3. Results and discussion

X-ray diffraction patterns of the ribbons in the as-cast state are shown in Fig. 1. The XRD patterns show the broad diffraction halo centered at about 3.1 $Å^{-1}$ that is typical for amorphous metallic alloys. No traces of crystalline precipitations have been detected. The measurements were carried out on the ribbon side that has no contact with the copper wheel.

Quantitative structural information about short-range ordering, i.e. the nearest-neighbors inter-atomic distances and the coordination numbers can be derived from the wide-angle X-ray scattering data. The scattering data are usually represented by the structure factor computed as

$$S(Q)=\frac{I(Q)-(\langle f^2\rangle-\langle f\rangle^2)}{\langle f\rangle^2}, \qquad (1)$$

where $\langle f^2\rangle=\sum_{i=1}^{n}c_i f_i^2$, and $\langle f\rangle=\sum_{i=1}^{n}c_i f_i$.

$I(Q)$ indicates the corrected and normalized intensity, c_i is the atomic concentration of the i-th element, f_i is the atomic scattering factor of the i-th kind element and n is the number of the atomic species in the sample. The values of the atomic scattering factors are tabulated in [10]. The structure factors for the investigated glasses are shown in Fig. 2. The presented diffraction data, consisting of a series of broad peaks, are typical for non-crystalline materials. Oscillations of the structure factors around the unity value are due to spatial correlations between atoms in the investigated sample. The present diffraction data are consistent with those reported in [11] obtained using electron diffraction.

The pair distribution function (PDF) can be obtained converting the scattering data to the real space representation via the sine Fourier transform as follows:

$$G(r)=4\pi r[\rho(r)-\rho_0]=\frac{2}{\pi}\int_0^{Q_{\max}}Q[S(Q)-1]W(Q)\sin(Qr)dr, \qquad (2)$$

where

$$W(Q)=\frac{\sin(\pi Q/Q_{\max})}{(\pi Q/Q_{\max})}$$

is the Lorch window function that minimize the truncation errors, Q_{max} is the maximum value of the scattering vector (here 22 $Å^{-1}$) and ρ_0 indicates the number density. For computing the integral in Eq. (2) the intensity data were smoothly extrapolated to the value of $Q=0$. The calculated PDFs are shown in Fig. 3. The physical meaning of the function $\rho(r)$ appearing in Eq. (2) is that $4\pi r^2\rho(r)dr$ represents the number of atoms in the spherical shell of the radius r and the thickness dr. Therefore the variable r represents the inter-atomic distance. From an inspection of Fig. 3, it can be concluded that the overall shape of the PDFs is similar and the presented plots exhibit very close features. It suggests the building units of the structure of the investigated glasses are very similar and decoration of atomic positions with Fe and Nb atoms depends on their concentration. In the other words in the $Fe_{70}Nb_{10}B_{20}$ and $Fe_{62}Nb_{8}B_{30}$ metallic glasses the Fe atoms are randomly substituted by Nb. From an inspection of Fig. 3 it can be seen that the peak positions of the PDF for the $Fe_{80}B_{20}$ glass are slightly shifted towards lower values of the inter-atomic distances when compared with the Nb containing samples. Such a tendency can be related to a larger radius of Nb in comparison with Fe. It is noteworthy that beyond the 18 Å limit there are no structural oscillations in the PDFs for the investigated glasses that indicates

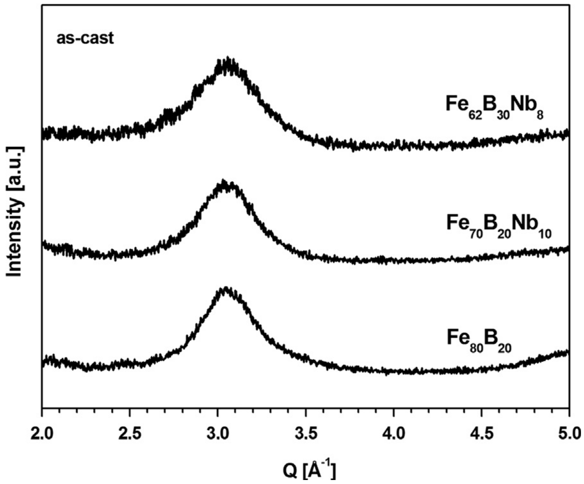

Fig. 1. X-ray diffraction patterns of studied $Fe_{80}B_{20}$, $Fe_{70}Nb_{10}B_{20}$ and $Fe_{62}Nb_{8}B_{30}$ glassy ribbons in as-cast state.

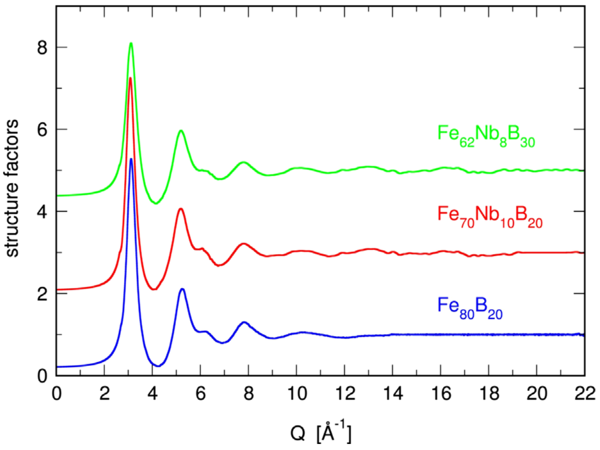

Fig. 2. Structure factors of $Fe_{80}B_{20}$, $Fe_{70}Nb_{10}B_{20}$ and $Fe_{62}Nb_{8}B_{30}$ metallic glasses.

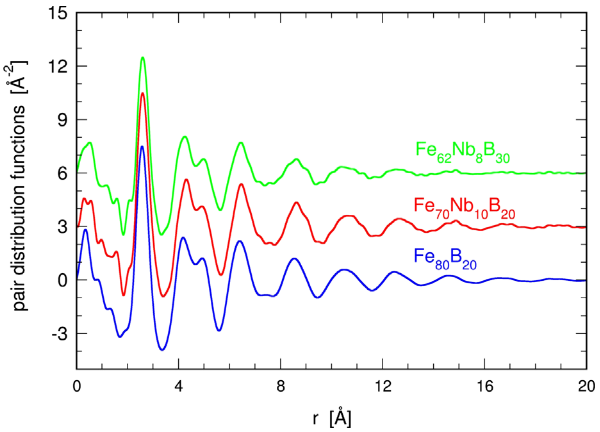

Fig. 3. Pair distribution functions of $Fe_{80}B_{20}$, $Fe_{70}Nb_{10}B_{20}$ and $Fe_{62}Nb_{8}B_{30}$ metallic glasses.